

# The Influence of pH and Halide Ions on Cefuroxime Electrochemical Degradation

Bogdan Tutunaru<sup>1,\*</sup> and Bogdan Oprea<sup>2,\*</sup>

<sup>1</sup> Department of Chemistry, Faculty of Sciences, University of Craiova, CUI: 4553380, Calea București 107i, 200478 Craiova, Dolj, Romania;

<sup>2</sup> Faculty of Medicine, University of Medicine and Pharmacy, Petru Rareș 2, 200349 Craiova, Dolj, Romania;

\*E-mail: [tutunaruchim@yahoo.com](mailto:tutunaruchim@yahoo.com); [oprea.bogdan@yahoo.com](mailto:oprea.bogdan@yahoo.com)

Received: 20 September 2021 / Accepted: 22 October 2021 / Published: 6 December 2021

---

An optimal combination of pH and halide ion is considered an effective strategy for the removal of cefuroxime from wastewater accrued from hospitals and clinical laboratories. A conventional electrochemical system with two platinum electrodes was used, and the electrolyte solution had different compositions and different pH values. The study of redox processes at the electrode / electrolyte interface was performed on the basis of cyclic voltammetry (CV) and constant current electrolysis supported by absorbance spectra obtained from UV–Vis spectrophotometry. The experimental results showed that the efficiency of antibiotic elimination can be increased to 100% in electrochemical systems by choosing the optimal parameters. Using the optimal conditions of the relevant factors, including the pH and nature of the anion, the degradation processes of cefuroxime in electrochemical systems are also compared by kinetic approach.

---

**Keywords:** cefuroxime; electrode processes; spectroelectrochemistry; electrodegradation

## 1. INTRODUCTION

Due to their spread in daily life, veterinary and environmental, cephalosporin antibiotics have been and are increasingly studied. The main issues of interest related to such antibiotics are: their use in improving the quality of life, ecotoxicity and human toxicity, the development of effective methods of determination, the study of physicochemical properties and the effectiveness of methods of cephalosporins degradation [1]. By changing the substituents in positions 3, 4 and 7 of the cephalosporin core, more than 50 antibiotics of this class are obtained, divided into first, second, third and fourth generations [1].

The solubility and bioavailability of cefuroxime raise major issues, and some studies improve these properties by esterification at the C4 position. Obtaining gastroretentive formulations of cefuroxime was tested in vivo [2]. Floating cefuroxime tablets have been formulated as an approach to increase gastric residence time and thus improve bioavailability [2]. Hydroxyapatite and  $\beta$ -tricalcium phosphate impregnated with cefuroxime were tested in vivo and in vitro for the treatment of osteomyelitis [3]. The study shows that these substances are effective carriers for antibiotics even for *Staphylococcus aureus* infections [3]. It has been shown that different conditions, such as nano-topography (nano-smooth, nano-rugged and nano-tubular), loading solution concentration ( $150 \text{ mg} \times \text{mL}^{-1}$  and  $25 \text{ mg} \times \text{mL}^{-1}$ ) and crystal structure (anatase and rutile), can influence the performance of titanium dioxide nanotubes carrying cefuroxime in the prevention of infections in the periprosthetic joints [4].

Antibiotics, including cephalosporins are typically administered to prevent or treat bacterial infections. Improper production, storage, marketing or use leads to their penetration into food or the environment, while excessive use results in increased antimicrobial resistance [1, 5]. Ultra-High Performance Liquid Chromatography (UHPLC) together with Mass Spectrometric detection (MS) has become the preferred technique for quantifying and confirming the presence of antibiotics in food [5–10]. The tandem of these methods has been successfully used in the identification and quantification of 12 penicillins, 12 cephalosporins (including cefuroxime) and 5 carbapenems in biological samples [5]. Monitoring of therapeutically administered drugs is a standard FDA guideline used to minimize toxicity and maximize drug efficacy. An ultrafast Hydrophilic-Interaction Chromatography (HILIC) based UPLC-MS/MS method was successfully used for the determination of 9  $\beta$ -lactam antibiotics in human plasma [6]. In fact, both antibiotics contaminate the environment, but also bioactive metabolites and their degradation products. It is also possible to determine both antibiotics and their transformation products simultaneously using UPLC-MS methods. Their knowledge can significantly improve the ability to control the efficiency of biological processes [7]. The spectrofluorimetric method proved to be sensitive enough to allow the determination of cefuroxime in very small quantities, with a detection limit of  $0.05\text{--}1.7 \text{ } \mu\text{g} \times \text{mL}^{-1}$  [11, 12].

Very low detection limits of  $7 \times 10^{-10} \text{ mol} \times \text{L}^{-1}$  have been reached for the determination of cefuroxime using adsorptive stripping voltammetry [13]. This method uses the complexation reactions of the antibiotic with the metal ions of Cd, Cu and Zn. Another electrochemical method, such as polarography, has been used to characterize cephalosporin antibiotics, including cefuroxime [14, 15].

During synthesis, storage, handling or use, antibiotics are emitted into the environment and from a useful compound they become pollutants [16–27]. Such environmental problems require the complete elimination of these toxic compounds from the environment [17–27]. Heterogeneous photocatalytic degradation [17], bioremediation using in vitro cultures (*Lentinula edodes* [18], *Bacillus clausii* [19], Xanthomonadaceae [20], coccoid and bacilliform bacteria [21]) are just a few methods used to degrade cefuroxime in polluted waters. Photoassisted ozonation [22], indirect and electromediated electrochemical degradation [23], advanced oxidation processes [24] or the use of oxidizing reagents such as  $\text{NaHCO}_3$  [25] and hexacyanoferrate (III) under alkaline conditions [26] are effective methods of cephalosporin removal from polluted waters.

The aim and the worth of the study are to evaluate the influence of the anion and the pH, respectively, on the electrochemical degradation of simulated waters polluted with cefuroxime. Very high pH values (close to alkaline drinking water) and very low (similar to the gastric environment) were chosen for an assessment as close as possible to certain possible biological conditions.

## 2. MATERIALS AND METHODS

### 2.1. Materials

Cefuroxime (CFRX) was purchased as a powder for I.M./I.V. injection in the form of single use vials with a mass of 750 mg / vial (Cefuroxime Atb®, Antibiotice a+). The active substance is cefuroxime sodium.

Alkaline halides namely sodium fluoride, sodium chloride and sodium bromide were used as the supporting electrolyte. They had purities higher than 99.5% (from MERCK, Germany) and were used in the conditions in which they were purchased.

Four stock solutions were prepared;  $8.8 \times 10^{-3} \text{ mol} \times \text{L}^{-1}$  CFRX;  $1.0 \text{ mol} \times \text{L}^{-1}$  NaF;  $1.0 \text{ mol} \times \text{L}^{-1}$  NaCl and  $1.0 \text{ mol} \times \text{L}^{-1}$  NaBr. The cefuroxime stock solution was maintained in dark and cold conditions. Sodium halide stock solutions were prepared for one working day and all were analyzed on the same day. Sodium halide solutions (electrolyte support solutions) and solutions containing both the supporting electrolyte and CFRX were analyzed spectroelectrochemically.

The working electrolyte solution contained the NaX support electrolyte at a concentration of  $0.1 \text{ mol} \times \text{L}^{-1}$  and the antibiotic at a concentration of  $8.8 \times 10^{-5} \text{ mol} \times \text{L}^{-1}$ .

$\text{H}_2\text{SO}_4$  and NaOH were used to adjust the pH to 2 and 12, respectively. Both sulfuric acid and sodium hydroxide were obtained from Fluka and had analytical purity. The pH value of 6.7 was the natural neutral value, without the addition of sulfuric acid or sodium hydroxide.

All solutions were prepared with distilled water and the analyses were performed at room temperature,  $22 \pm 2 \text{ }^\circ\text{C}$ .

### 2.2. Methods and procedures

Both Cyclic Voltammetry (CV) and electrolysis at constant current density were performed using VoltaLab 40 electrochemical research equipment [27–32]. This instrumentation was controlled by a computer using VoltaMaster 4 software. Electrochemical measurements were performed in a dynamic regime; this involves stirring the solution with a magnetic stirrer (stirring rate equal to 300 rpm). The two electrodes (working electrode and counter electrode) were made of platinum and had a geometric area of 1 square centimeter. The experimental values were recorded in relation to a reference electrode consisting of the Ag|AgCl,KCl sat electrode. The cyclic voltammograms of all the studied electrolytic systems were acquired with a potential sweep of  $100 \text{ mV} \times \text{s}^{-1}$ .

UV–Vis spectrophotometric analysis of working solutions was performed using a Varian Cary 50 Conc UV–Vis Photometer [27–32]. The spectrophotometer includes a 10mm quartz cuvette.

The influence of pH on the electrolyte / electrode interface processes was studied at three different values (2; 6.7; 12). The pH measurement was performed with a Hanna Instruments pH meter.

100 mL of  $0.1 \text{ mol}\times\text{L}^{-1}$  solutions of sodium fluoride, sodium chloride and sodium bromide (NaX) were prepared using appropriate stock solutions with a concentration of  $1.0 \text{ mol}\times\text{L}^{-1}$ . 100 mL of  $0.1 \text{ mol}\times\text{L}^{-1}$  NaX solution (NaF, NaCl and NaBr) containing  $8.8\times 10^{-5} \text{ mol}\times\text{L}^{-1}$  CFRX were also prepared using appropriate stock solutions. These solutions were subjected to electrochemical analysis (cyclic voltammetry and electrolysis at constant current density). A freshly prepared working solution was used in each electrochemical analysis.

The support electrolyte solutions ( $0.1 \text{ mol}\times\text{L}^{-1}$  NaF;  $0.1 \text{ mol}\times\text{L}^{-1}$  NaCl;  $0.1 \text{ mol}\times\text{L}^{-1}$  NaBr), as well as the NaBr\_CFRX solution, were electrolyzed for 15 minutes; the NaCl\_CFRX solution was electrolyzed for 30 minutes, and the NaF\_CFRX solution was electrolyzed for 60 minutes. Starting with the initial moment (zero electrolysis time) and later, at different times, 3 mL of solution was taken and subjected to spectrophotometric analysis.

The spectrophotometric analysis of the solutions was performed in the wavelength range of 200–800 nm. No molecular absorption phenomena were recorded at wavelength values greater than 600 nm, for this reason the graphs are represented in the range 200–600 nm.

### 3. RESULTS AND DISCUSSION

#### 3.1. Electrochemistry of support electrolyte solution

Figure 1 shows the cyclic voltammetry responses obtained for the electrochemical systems represented by the platinum electrodes in support electrolytes solutions ( $0.1 \text{ mol}\times\text{L}^{-1}$  NaF;  $0.1 \text{ mol}\times\text{L}^{-1}$  NaCl;  $0.1 \text{ mol}\times\text{L}^{-1}$  NaBr) used in the study. This study was performed at different pH values, under the same conditions in which the electrode processes of the antibiotic were studied (pH = 2; 6.7 and 12). To make a clear distinction between the electrode processes attributed to the supporting electrolyte and those of the biologically active compound cefuroxime (CFRX), cyclic voltammograms were recorded and are illustrated in Figure 1.

As can be seen in Figure 1, at low values of the working electrode potential, no significant distinction can be made between the electrochemical response of the NaF system in a neutral and alkaline environment. At the same time, at high values of the working electrode potential, no clear distinction can be made between the electrochemical responses of the system in neutral and acidic environment. As the potentials move to more positive values, small oscillations of anodic current densities are recorded due to the adsorption of hydroxyl ions on the working electrode surface [33–36]. Another important aspect to consider is that, starting with the potentials of  $-0.8 \text{ V}$ , the formation of oxy/hydroxy /oxyhydroxides takes place on the surface of the platinum electrode [33–36].

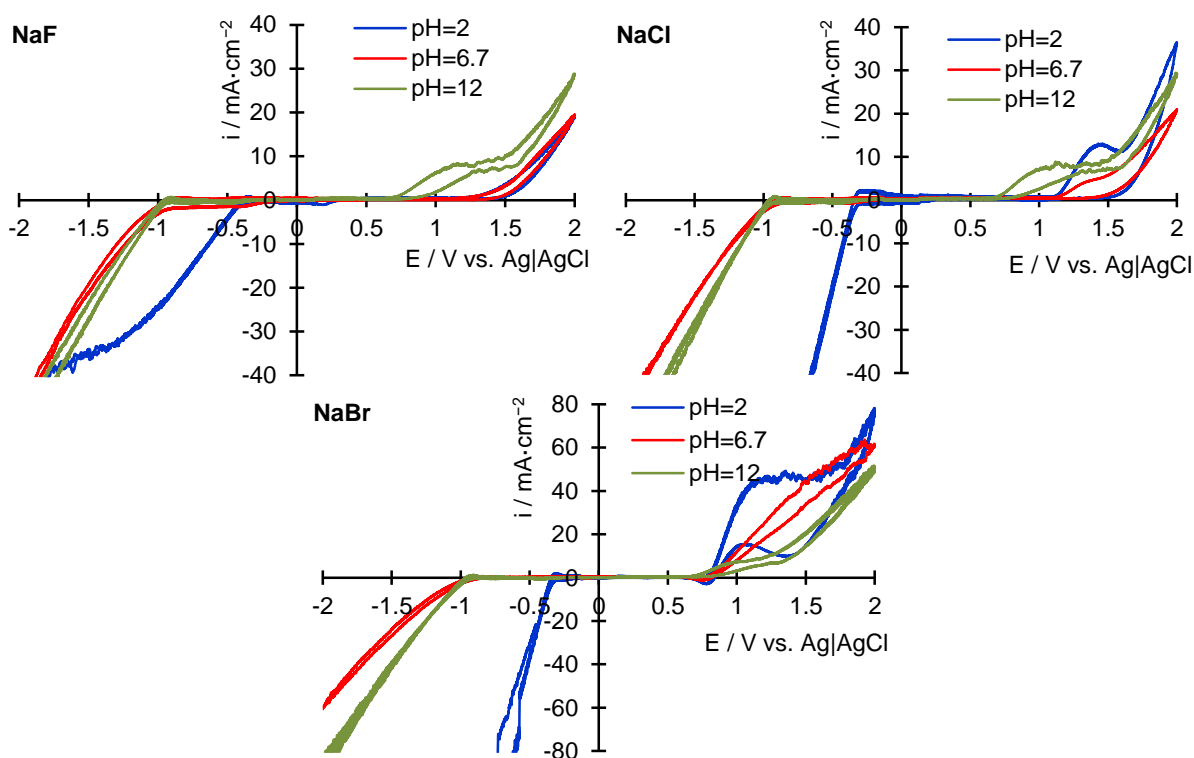


**Figure 1.** Cyclic voltammetry responses of platinum electrode in  $0.1 \text{ mol}\times\text{L}^{-1}$  NaF;  $0.1 \text{ mol}\times\text{L}^{-1}$  NaCl and  $0.1 \text{ mol}\times\text{L}^{-1}$  NaBr at different values of pH.

In the field of anodic current densities and at potentials higher than 0.75 V, there is a significant increase of the current densities associated with the processes of formation of surface oxides in a higher oxidation state and implicitly with the oxygen evolution reaction. In an alkaline environment the anodic current densities have the highest values, unlike the acidic and neutral environments in which lower values are recorded correlated with the smallest hysteresis area. Experimental observations can thus be correlated with the electrode processes, namely in the anodic field the main process is the oxygen evolution reaction [33–36], and in an alkaline environment the current densities are the highest. A high concentration of protons in the environment leads, experimentally, to an increase in cathodic current densities, and this process is attributed to the hydrogen evolution reaction.

Cyclic voltammetry response of the electrochemical system consisting of platinum electrodes immersed in the NaCl solution as a support electrolyte indicates similar experimental results of the cathodic behavior. In an acidic environment, the chloride ion is involved in the electrode processes, oxidizes and leads to the formation of oxychlorinated ionic species [37, 38] (Table 1; Figure 1–NaCl). These processes are identified experimentally and correspond to the anodic peak at 1.4 V. In an acidic environment, the electrochemical processes of the chloride-containing electrolyte solution are very complex, as illustrated by the possible reactions in Table 1.

According to the comparative cyclic voltammograms of the electrochemical system containing chloride, the highest values of current densities are obtained in acidic medium; thus, it can be concluded that the high concentration of protons favors the formation of active oxychlorinated species. In an alkaline environment, the experimental results are similar to the previous case, with the

difference that the oxychlorinated species are electrochemically generated at lower values of the working electrode potentials (corresponding to the reactions in Table 1 – alkaline medium).

**Table 1.** Oxy-Chlorine ions reactions in acidic and alkaline medium.

Acidic medium		Alkaline medium	
reaction	E / V	reaction	E / V
$\text{ClO}_3^- + 2\text{H}^+ + 2e \rightarrow \text{ClO}_2 + \text{H}_2\text{O}$	1.13/1.175	$\text{ClO}_4^- + \text{H}_2\text{O} + 2e \rightarrow \text{ClO}_3^- + 2\text{HO}^-$	0.17
$\text{ClO}_3^- + 3\text{H}^+ + 2e \rightarrow \text{HClO}_2 + \text{H}_2\text{O}$	1.157/1.181	$\text{ClO}_3^- + \text{H}_2\text{O} + 2e \rightarrow \text{ClO}_2^- + 2\text{HO}^-$	0.35
$\text{ClO}_2 + \text{H}^+ + e \rightarrow \text{HClO}_2$	1.19/1.068	$2\text{ClO}^- + 2\text{H}_2\text{O} + 2e \rightarrow \text{Cl}_2 + 4\text{HO}^-$	0.421
$\text{ClO}_4^- + 2\text{H}^+ + 2e \rightarrow \text{ClO}_3^- + \text{H}_2\text{O}$	1.19÷1.226	$\text{ClO}_2^- + \text{H}_2\text{O} + 2e \rightarrow \text{ClO}^- + 2\text{HO}^-$	0.59
$\text{Cl}_2 + 2e \rightarrow 2\text{Cl}^-$	1.39	$\text{ClO}_3^- + 3\text{H}_2\text{O} + 6e \rightarrow \text{Cl}^- + 6\text{HO}^-$	0.622
$\text{ClO}_3^- + 6\text{H}^+ + 6e \rightarrow \text{Cl}^- + 3\text{H}_2\text{O}$	1.45	$\text{ClO}^- + \text{H}_2\text{O} + 2e \rightarrow \text{Cl}^- + 2\text{HO}^-$	0.89
$2\text{ClO}_3^- + 12\text{H}^+ + 10e \rightarrow \text{Cl}_2 + 6\text{H}_2\text{O}$	1.49		
$\text{HClO} + \text{H}^+ + 2e \rightarrow \text{Cl}^- + \text{H}_2\text{O}$	1.49		
$2\text{HClO} + 2\text{H}^+ + 2e \rightarrow \text{Cl}_2 + 2\text{H}_2\text{O}$	1.63		
$\text{HClO}_2 + 2\text{H}^+ + 2e \rightarrow \text{HClO} + \text{H}_2\text{O}$	1.67		

Bromide is also an electrochemically active ion [39–41], and its participation in interface processes is also influenced by the concentration of protons (Figure 1 – NaBr and Table 2). The electrochemical behavior of this system has two obvious characteristics: i) both anodic and cathodic current densities have the highest values, ii) at a high concentration of protons, the cyclic voltammetry response has the largest hysteresis cycle, which means a higher susceptibility to oxidation.

**Table 2.** Oxy-Bromine ions reactions in acidic and alkaline medium.

Acidic medium		Alkaline medium	
reaction	E / V	reaction	E / V
$\text{Br}_2 + 2e \rightarrow 2\text{Br}^-$	1.078/1.087	$2\text{BrO}^- + 2\text{H}_2\text{O} + 2e \rightarrow \text{Br}_2 + 4\text{HO}^-$	0.455
$\text{HBrO} + \text{H}^+ + 2e \rightarrow \text{Br}^- + \text{H}_2\text{O}$	1.341	$\text{BrO}_3^- + 3\text{H}_2\text{O} + 6e \rightarrow \text{Br}^- + 6\text{HO}^-$	0.613/0.584
$\text{BrO}_3^- + 5\text{H}^+ + 4e \rightarrow \text{HBrO} + 2\text{H}_2\text{O}$	1.45/1.49	$\text{BrO}^- + \text{H}_2\text{O} + 2e \rightarrow \text{Br}^- + 2\text{HO}^-$	0.766
$\text{BrO}_3^- + 6\text{H}^+ + 6e \rightarrow \text{Br}^- + 3\text{H}_2\text{O}$	1.478	$\text{HBrO} + 2e \rightarrow \text{Br}_2 + 2\text{HO}^-$	1.604
$\text{BrO}_3^- + 12\text{H}^+ + 10e \rightarrow \text{Br}_2 + 6\text{H}_2\text{O}$	1.48÷1.513		
$\text{BrO}_4^- + 2\text{H}^+ + 2e \rightarrow \text{BrO}_3^- + \text{H}_2\text{O}$	1.85 V		

At potentials higher than 1.0 V, bromide ions participate in oxidative electrotransformation processes with the generation of oxybrominated ions [39–41], which are strong oxidizing agents.

As a conclusion of the results provided by cyclic voltammetry, it can be stated that in the presence of the inert fluoride ion, the predominant processes of the electrode are represented by the hydrogen and oxygen evolution reactions, and in the case of solutions containing chloride or bromide ions, the anodic processes are represented by the electrogeneration of oxyhalogenated species and the cathodic processes by the hydrogen evolution reaction.

Understanding the electrode / electrolyte interface processes of the supporting electrolyte and subtracting them from the electrode processes of cefuroxime allows elucidation of the electrotransformation processes in which the antibiotic participates.

Complementary to the analysis of cyclic voltammetry, these systems were analyzed by constant current electrolysis in association with UV–Vis spectrophotometry [23, 27, 37, 38] at different times and different pH values (Figure 2). The UV–Vis spectra shown in Figure 1 are recorded in the presence of the NaF support electrolyte, and the absorbance values are constant and low, they are also invariant in terms of time and pH variation (Figure 2 - NaF). Spectrophotometric analysis demonstrates the inertia of the fluorine ions and certifies the results obtained by cyclic voltammetry.

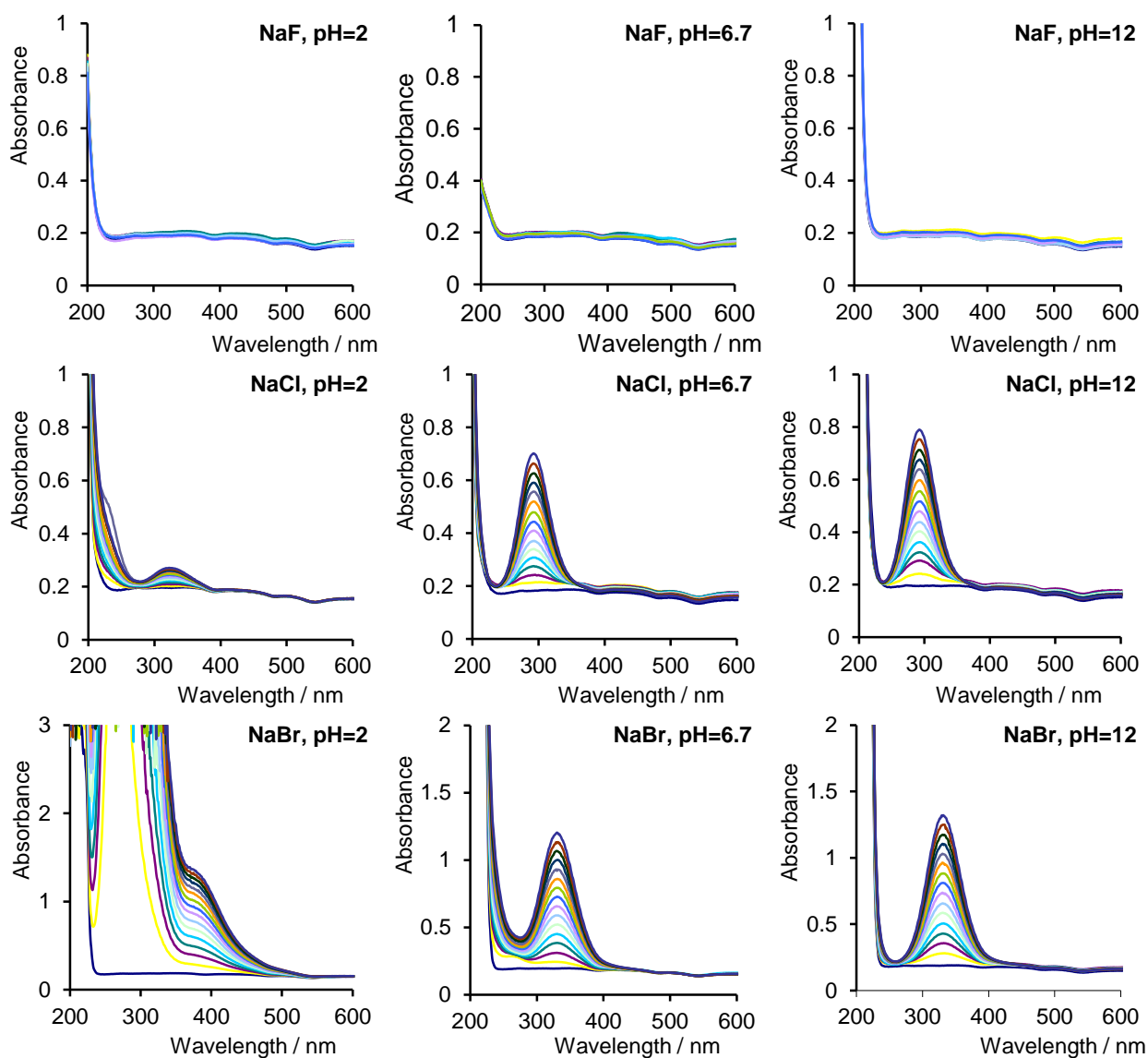


**Figure 2.** UV–Vis absorption spectra of support electrolyte solution (NaF, NaCl and NaBr systems) as the constant current electrolysis progress over time at different values of pH (current density =  $50 \text{ mA} \times \text{cm}^{-2}$ ).

The electrochemical response obtained for chloride ions is edifying for electrogenerated oxychlorinated species. At a pH close to neutral (6.7), the UV–Vis spectrum has a maximum absorption at the wavelength of 290 nm [23, 27]. The absorbance values corresponding to this peak

increase over time, so that over time there is an increase in the concentration of oxychlorinated species in the solution. In an alkaline environment the processes are similar, so that the absorption peak is recorded at 290 nm and has an even higher intensity (Figure 2 – NaCl, pH = 6.7 and 12). The high concentration of protons changes both the state of the surface and the mechanisms of the electrode processes, which leads to the electrogeneration of chemical species different from previous cases. The high concentration of protons changes both the state of the surface and the mechanisms of the electrode processes, which leads to the electrogeneration of chemical species different from previous cases.

The increase in absorbance at wavelengths less than 250 nm and 320 nm highlights the formation of species that have not been identified in a neutral or alkaline environment.

The results of the cyclic voltammetry analysis are corroborated by those obtained by spectrophotometry. The electrochemical system containing bromide ions shows a similar behavior in neutral and alkaline medium (Figure 2 – NaBr, pH = 6.7 and 12). Under these conditions, the electrogenerated compounds from the redox processes at the electrode / electrolyte interface are identified at a wavelength of 330 nm. In a strongly acidic environment with pH = 2, oxybrominated species are also identified, but are different and attributed to the very high intensity peak at 280 nm and the low intensity peak at 380 nm (Figure 2 – NaBr, pH = 2).

### 3.2. Electrochemistry of CFRX electrolyte solution. Influence of halide ion and different pH values

The aspects of molecular electrochemistry involve the study of the electrode processes in which the molecular compound participates, but also the direct, indirect or mediate influence of the supporting electrolyte [42–44]. Figure 3 illustrates the cyclic voltammetry response of the electrochemical systems represented by support electrolyte solutions that also contain the antibiotic, to different pH values.

The presence of the antibiotic in the working solution and at a neutral pH changes both the anodic and the cathodic behavior. Under these conditions, the cathodic current densities indicate the appearance of a new peak (Figure 3 – NaF\_CFRX), at the potential of  $-0.9$  V, in the form of a shoulder, slightly wide and of low intensity. Also, in a neutral environment and at high anodic overvoltages, the values of current densities decrease from 20 (Figure 1 – NaF) to  $15 \text{ mA} \times \text{cm}^{-2}$ ; effects due to the strong adsorption processes of cefuroxime on the electrode surface. In this potential range, the electrochemical behavior at pH = 2 is similar to that at pH = 6.7, with the same observation that current densities have a decreasing tendency. An opposite effect is observed in an alkaline environment, where the increase of anodic and cathodic current densities is registered, an effect associated with an increase of the hysteresis cycle by extracting the effect of the supporting electrolyte.

For the electrochemical system containing chloride ions, there is a decrease in anodic current densities in acidic medium and an intensification of anodic processes in neutral and alkaline medium, respectively. The observed behavior is a cumulative one of the processes in which the supporting electrolyte and the antibiotic participate. A correct interpretation must take into account: the processes of electrogeneration of the oxychlorinated species corresponding to the pH used (according to Figure 1



– NaCl); participation of these species in electrotransformation processes (chloride / chlorite / chlorate / perchlorate); the reaction, in homogeneous phase – inside the solution, between these species and the antibiotic molecules [23, 37, 38]

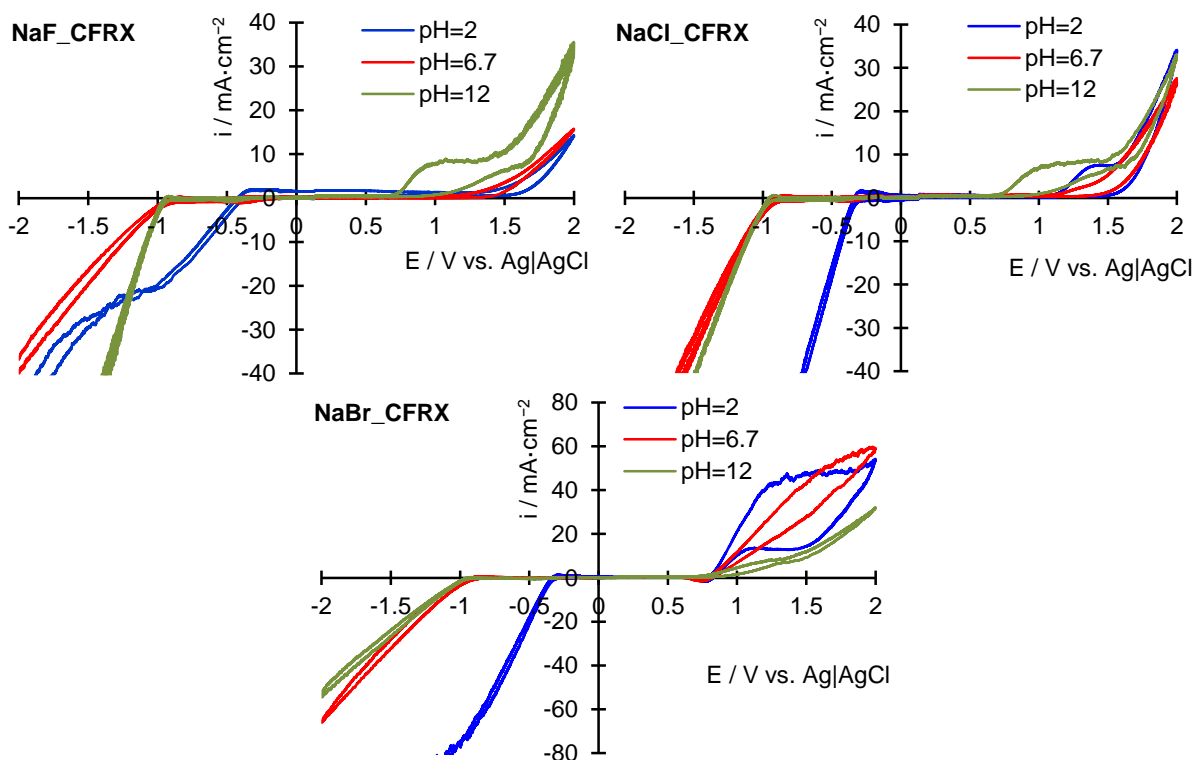


**Figure 3.** Cyclic voltammety responses of platinum electrode in  $0.1 \text{ mol}\times\text{L}^{-1}$  NaF;  $0.1 \text{ mol}\times\text{L}^{-1}$  NaCl and  $0.1 \text{ mol}\times\text{L}^{-1}$  NaBr containing  $8.8\times 10^{-5} \text{ mol}\times\text{L}^{-1}$  CFRX at different values of pH (sweep rate =  $100 \text{ mV}\times\text{s}^{-1}$ ).

By replacing the support electrolyte anion with bromide, a change in the characteristics of the cyclic voltammograms is noticed. Bromide ions are oxidized anodically in acidic medium (Figure 1 – NaBr), and the anodic current density has the highest values of  $80 \text{ mA}\times\text{cm}^{-2}$ . This value is significantly reduced when the antibiotic is added to the solution. In an environment close to the natural neutral pH, the sensitivity to oxidation increases, and in an alkaline environment the densities of the anodic current decrease from 50 (Figure 1) to about  $30 \text{ mA}\times\text{cm}^{-2}$  (Figure 3).

The study of the electrode processes of cefuroxime was performed by spectroelectrochemical methods, which involved a tandem of two techniques, namely constant current electrolysis and UV–Vis spectrophotometry analysis (Figure 4) [32, 37, 38].

The UV–Vis molecular absorption spectrum of cefuroxime (Figure 4 – NaF\_CFRX) is characterized by a UV maximum absorption at the wavelength of 276 nm, invariant with the pH value. During the 60–minute electrolysis period, the electrochemical system containing NaF and CFRX indicates a continuous and constant decrease in maximum absorption values. This behavior is attributed to the electrochemical degradation of polluting molecules by a direct mechanism on the

electrode surface. The decrease in absorbance is thus correlated with the decrease in the concentration of cefuroxime in solution. Another important feature is that no other maximum absorption is recorded in the analyzed UV–Vis range; a direct consequence is that the degradation does not generate spectrophotometrically active intermediate or final degradation products [23, 27].

In the presence of the electroactive chloride ion, the processes are different from the previous case and are also pH dependent. The spectroelectrochemical study of this system was performed over a period of 15 minutes; the spectra being recorded every minute.

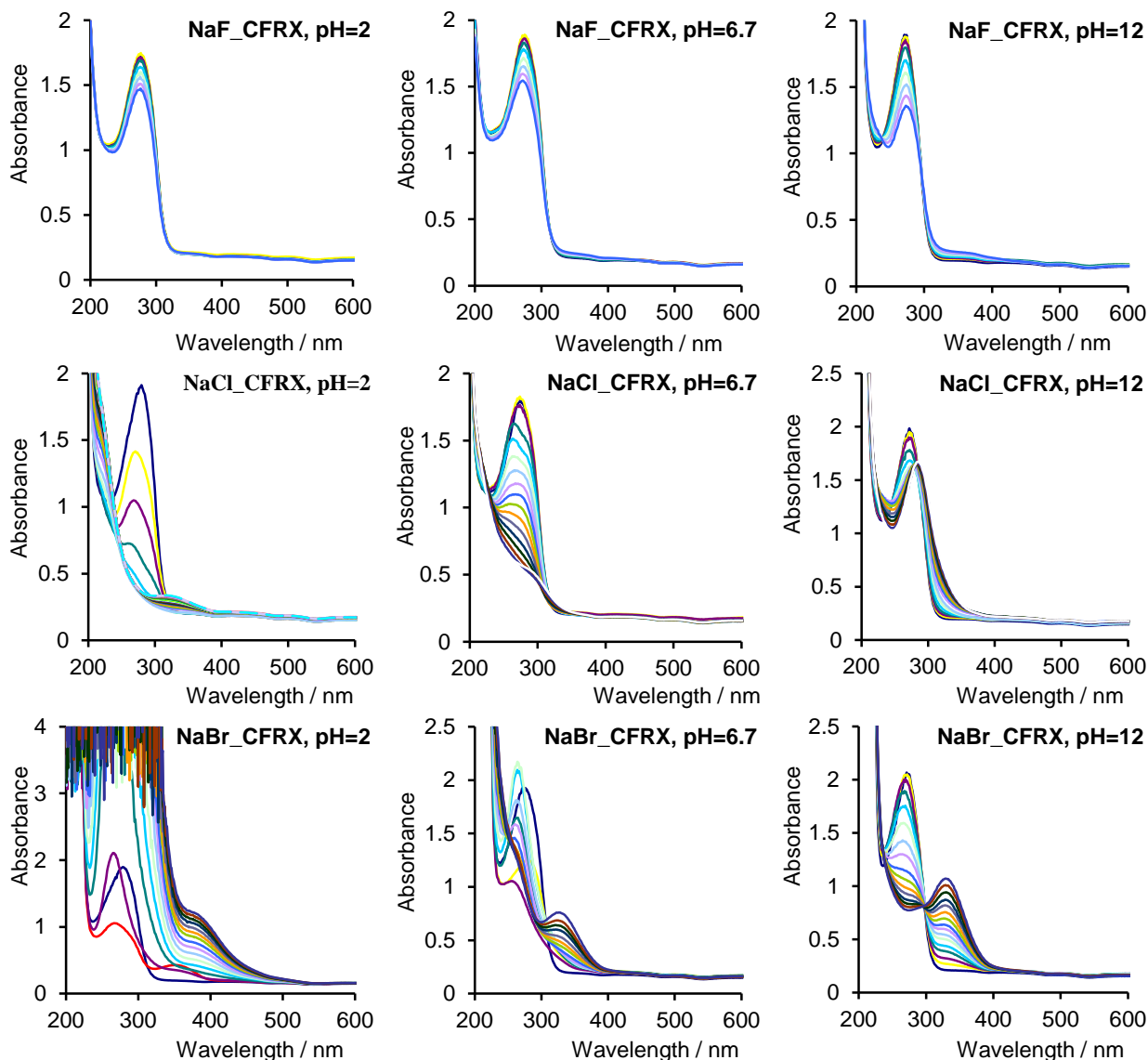


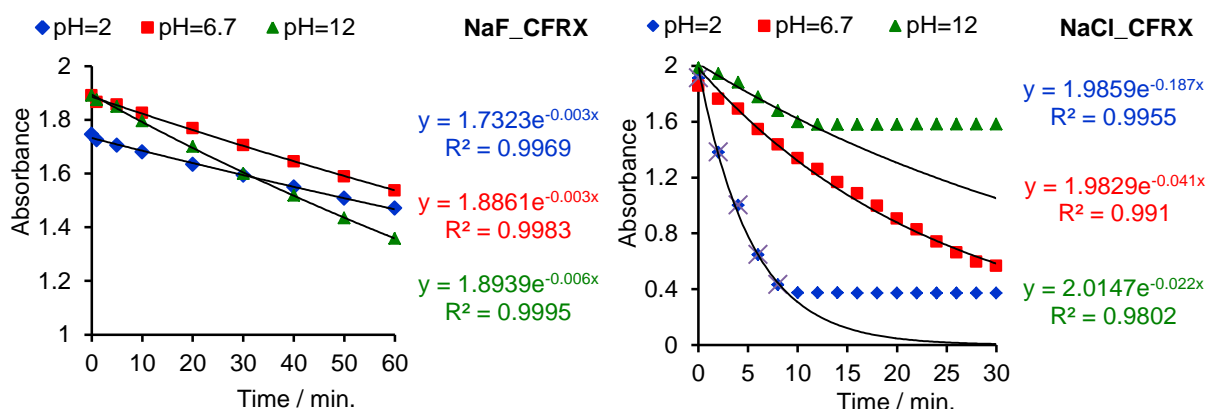
**Figure 4.** UV–Vis absorption spectra of work electrolyte solutions containing both  $0.1 \text{ mol} \times \text{L}^{-1}$  NaF/NaCl/NaBr and  $8.8 \times 10^{-5} \text{ mol} \times \text{L}^{-1}$  CFRX as the constant current electrolysis progress over time at different values of pH ( $i = 50 \text{ mA} \times \text{cm}^{-2}$ ).

A high concentration of hydrogen ions (Figure 4, NaCl\_CFRX, pH = 2), leads to a rapid decrease in cefuroxime absorbance, as indicated by the corresponding UV spectrum. A closer analysis of the UV spectrum at the detection limit of the photometer (wavelengths less than 220 nm) shows a slight increase in absorbance simultaneously with the appearance of a maximum absorption at 320 nm, which confirms the formation of oxychlorinated species (Figure 2). At a pH close to neutral, a decrease in absorbance is observed, but slower, in this case, the electrogenerated species are consumed by reactions in the homogeneous phase, as they are electrogenerated. In an alkaline environment the degradation is partial and is recorded only in the first 10 minutes of electrolysis. After this time, the absorbance attributed to CFRX molecules is constant, simultaneously with a slow increase in absorption at wavelengths of 320–360 nm.

Bromide ions and the corresponding oxybrominated species determine the evolution of the process by other mechanisms (Figure 4, NaBr\_CFRX). In acidic environment from the first minutes of electrolysis there is a rapid alteration of both the wavelength and the maximum absorbance. After subtracting the electrode processes attributed to the supporting electrolyte (Figure 2), the electrochemical degradation of cefuroxime molecules in acidic medium is the fastest. The change in the absorption wavelength may be due to changes in both the electronic and chemical structure of the cefuroxime molecule [23]. In an alkaline environment, as the concentration of cefuroxime decreases due to degradation at the electrode surface, there is also an increase in the concentration of electrogenerated bromide species, marked by an isosbestic point at 300 nm.

### 3.3. Kinetics of electrochemical processes

The kinetic approach allowed the quantitative evaluation of the degradation processes of cefuroxime under the studied experimental conditions [23, 31, 32]. Figure 5 shows the variations of absorbance for each of the studied electrochemical systems.



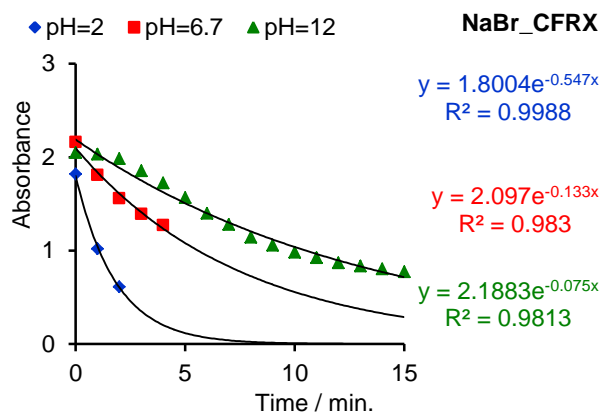


**Figure 5.** Time variation of absorbance values for NaX\_CFRX electrochemical systems during constant current electrolysis. Pt electrodes; X = F, Cl, Br; pH = 2, 6.7, 12;  $i = 50 \text{ mA} \times \text{cm}^{-2}$ .

The rate law for electrochemical reactions correlates the rate of reaction with the concentrations / absorbance of the reactants. Using the integrated form of the first order reaction rate law ( $A = A_0 \cdot e^{-kt}$ ), the rate constant was obtained for each electrochemical system studied using the graphical method (Figure 5, Table 3).

**Table 3.** Electrochemical degradation rates ( $\text{min}^{-1}$ ) of Cefuroxime in the presence of different support electrolyte and different pH values.

support electrolyte	pH = 2	pH = 6.7	pH = 12
NaF	0.003	0.003	0.006
NaCl	0.187	0.041	0.022
NaBr	0.547	0.133	0.075

When the solution contains the inert support electrolyte NaF, the rate constant has the lowest values ( $0.003/0.006 \text{ min}^{-1}$ ), regardless of the pH of the medium. By simply changing the fluoride ion with chloride, the rate constants increase greatly. Thus, in acid medium the value reaches  $0.187 \text{ min}^{-1}$ , which is 62 times higher. There are two reasons for this increase: i) a high concentration of hydrogen ions favors the formation of ionic species of the cefuroxime molecule, or at least the increase in the polarizability of this molecule which results in faster degradation; ii) a high concentration of hydrogen ions favors the formation of oxychlorinated species which are stronger oxidants [31, 37, 38]. The capacity of oxybrominated species on the electrochemical degradation of cefuroxime is given by the increase of the rate constant to  $0.547 \text{ min}^{-1}$ , in acidic environment.

#### 4. CONCLUSIONS

The application of modern UV-Vis spectroelectrochemistry techniques for pharmaceutical analysis can be achieved with resounding success. The electrochemical behavior of cephalosporin

cefuroxime was evaluated by cyclic voltammetry using platinum electrodes, and the influence of the halide anion and the pH of the solution were investigated by spectroelectrochemistry.

The association of electrochemical methods with spectrophotometric analysis demonstrates the in situ electrogeneration of oxychlorinated and oxybrominated species. This is the reason why in the NaF\_CFRX system the molecular electrochemical processes take place through a direct mechanism, while in the NaCl\_CFRX and NaBr\_CFRX systems the processes take place through an indirect and / or electromediated mechanism.

Quantitative evaluation of electrochemical processes by a kinetic approach demonstrates that the rate of electrochemical degradation has the highest value in the presence of bromide ion and a high concentration of protons.

#### ACKNOWLEDGMENTS

The funding of this work was supported by the research grants awarded by the University of Craiova, Romania, in the competition “The Awards of Research Results–ISI Articles”.

#### References

1. A. R. Ribeiro, B. Sures and T. C. Schmidt, *Environ. Pollut.*, 241 (2018) 1153.
2. G. K. Rao, P. K. Mandapalli, R. Manthri and V. P. Reddy, *Saudi Pharm. J.*, 21 (2013) 53.
3. S. K. Nandi, B. Kundu, S. K. Ghosh, T. K. Mandal, S. Datta, D. K. De and D. Basu, *Ceram. Int.*, 35 (2009) 1367.
4. P. Chennell, E. Feschet–Chassot, T. Devers, K. O. Awitor, S. Descamps and V. Sautou, *Int. J. Pharm.*, 455 (2013) 298.
5. M. Di Rocco, M. Moloney, T. O’Beirne, S. Earley, B. Berendsen, A. Furey and M. Danaher, *J. Chromatogr. A*, 1500 (2017) 121.
6. A. Abdulla, S. Bahmany, R. A. Wijma, B. C. H. van der Nagel and B. C. P. Koch, *J. Chromatogr. B*, 1060 (2017) 138.
7. S. Bajkacz, E. Felis, E. Kycia–Słocka, M. Harnisz, E. Korzeniewska, *Sci. Total Environ.*, 726 (2020) 138071.
8. N. O. Can, G. Altiokka and H. Y. Aboul–Enein, *Anal. Chim. Acta*, 576 (2006) 246.
9. P. Partani, S. Gurule, A. Khuroo, T. Monif and S. Bhardwaj, *J. Chromatogr. B*, 878 (2010) 428.
10. I. Ivana, Z. Ljiljana and Z. Mira, *J. Chromatogr. A*, 1119 (2006) 209.
11. M. A. Omar, O. H. Abdelmageed and T. Z. Attia, *Talanta*, 77 (2009) 1394.
12. J. A. Murillo, J. M. Lemus and L. F. Garcia, *J. Pharmaceut. Biomed.*, 12 (1994) 875.
13. N. A. El–Maali, A. H. Osman, A. A. M. Aly and G. A. A. Al–Hazmi, *Bioelectrochemistry*, 65 (2005) 95.
14. A. G. Fogg and N. M. Fayad, *Anal. Chim. Acta*, 108 (1979) 205.
15. F. I. Sengun, K. Ulas and I. Fedai, *J. Pharmaceut. Biomed.*, 3 (1985) 191.
16. V. Chigor, I. A. Ibangha, C. Chigor and Y. Titilawo, *Heliyon*, 6 (2020) e03780.
17. A. Pourtaheri and A. Nezamzadeh–Ejhih, *Spectrochim. Acta A*, 137 (2015) 338.
18. M. Dąbrowska, B. Muszyńska, M. Starek, P. Żmudzki and W. Opoka, *Int. Biodeter. Biodegr.*, 127 (2018) 104.
19. X. X. Kong, J. L. Jiang, B. Qiao, H. Liu, J. S. Cheng and Y. J. Yuan, *Sci. Total Environ.*, 651 (2019) 271.
20. Z. Cheng, X. Hu and Z. Sun, *Chem. Eng. J.*, 303 (2016) 137.
21. Z. Cheng and X. Hu, *Chem. Eng. J.*, 320 (2017) 93.

22. R. R. Solís, A. M. Chavez, O. Monago–Marana, A. Munoz de la Pena and F. J. Beltran, *Sep. Purif. Technol.*, 266 (2021) 118514.
23. B. Tutunaru, A. Samide, S. Iordache, C. Tigae, A. Simionescu and A. Popescu, *Appl. Sci.–Basel*, 11 (2021) 1376.
24. R. Anjali and S. Shanthakumar, *J. Environ. Manage.*, 246 (2019) 51.
25. L. Zhang, R. Guo, H. Li, Q. Du, J. Lu, Y. Huang, Z. Yan and J. Chen, *J. Hazard. Mater.*, 394 (2020) 122531.
26. A. A. P. Khan, A. M. Asiri, A. Khan, N. Azum, M. A. Rub, M. M. Rahman, S. B. Khan, K. S. Siddiqi and K. A. Alamry, *J. Ind. Eng. Chem.*, 19 (2013) 595.
27. S. Iordache, B. Tutunaru, A. Samide, C. Tigae, A. Simionescu, A. Popescu, *Int. J. Electrochem. Sci.*, 16 (2021) 210346.
28. B. Tutunaru, A. Samide, A. Moanta, C. Ionescu and C. Tigae, *Int. J. Electrochem. Sci.*, 10 (2015) 223.
29. A. Samide, B. Tutunaru, C. Tigae, R. Efrem, A. Moanta and M. Dragoi, *Environ. Prot. Eng.*, 40 (2014) 93.
30. A. Samide, M. Dumitru, A. Ciuciu, B. Tutunaru and M. Preda, *Stud. U. Babes–Bol. Chem.*, 54 (2009) 157.
31. B. Tutunaru, C. Tigae, C. Spînu and I. Prunaru, *Int. J. Electrochem. Sci.*, 12 (2017) 396.
32. A. Samide, B. Tutunaru, R. M. Varut and B. Oprea, *Pharmaceuticals*, 14 (2021) 619.
33. B. Jayasankar and K. Karan, *Electrochim. Acta*, 273 (2018) 367.
34. S. G. Rinaldo, W. Lee, J. Stumper and M. Eikerling, *Electrocatalysis*, 5 (2014) 262.
35. L. Coustan, G. Shul and D. Bélanger, *Electrochem. Commun.*, 77 (2017) 89.
36. M. Alsabet, M. Grden and G. Jerkiewicz, *J. Electroanal. Chem.*, 589 (2006) 120.
37. B. Tutunaru, A. Samide, C. Neamtu and C. Tigae, *Int. J. Electrochem. Sci.*, 13 (2018) 5850.
38. A. Samide and B. Tutunaru, *Electroanal.*, 29 (2017) 2498.
39. X. Huang, Y. Qu, C. A. Cid, C. Finke, M. R. Hoffmann, K. Lim and S. C. Jiang, *Water Res.*, 92 (2016) 164.
40. M. Mastragostino and C. Gramellini, *Electrochim. Acta*, 30 (1985) 373.
41. A. R. Denaro, A. Mitchell and M. R. Richardson, *Electrochim. Acta*, 16 (1971) 755.
42. B. Ogorevc and S. Gomiscek, *J. Pharmaceut. Biomed.*, 9 (1991) 225.
43. B. Feier, A. Gui, C. Cristea and R. Sandulescu, *Anal. Chim. Acta*, 976 (2017) 25.
44. S. E. Kablan and N. Özaltın, *J. Electroanal. Chem.*, 785 (2017) 144.